Published OnlineFirst May 12, 2009; DOI: 10.1158/1535-7163.MCT-08-1098

Synthesis and characterization of a high-affinity $\alpha_v\beta_6$-specific ligand for *in vitro* and *in vivo* applications

Shunzi Li,[1] Michael J. McGuire,[1] Mai Lin,[2] Ying-Horng Liu,[1] Tsukasa Oyama,[1] Xiankai Sun,[2] and Kathlynn C. Brown[1]

[1]Division of Translational Research, Department of Internal Medicine, Simmons Comprehensive Cancer Center and [2]Department of Radiology, University of Texas Southwestern Medical Center, Dallas, Texas

Abstract

The $\alpha_v\beta_6$ integrin is an attractive therapeutic target for several cancers due to its role in metastasis and its negligible expression in normal tissues. We previously identified a peptide from a phage-displayed peptide library that binds specifically to $\alpha_v\beta_6$. The tetrameric version of the peptide has higher affinity for its cellular targets than the corresponding monomers. However, the inefficient synthesis limits its clinical potential. We report here a convergent synthesis producing the tetrameric peptide in high yield and purity. The ease of the synthesis allows for rapid optimization of the peptide. We have optimized this $\alpha_v\beta_6$ integrin–binding peptide, determining the minimal binding domain and valency. Importantly, the half-maximal binding affinity of the optimal peptide for its target cell is in the 40 to 60 pmol/L range, rivaling the affinity of commonly used antibody-targeting reagents. This peptide mediates cell-specific uptake, is functional in diagnostic formats, is stable in sera, and can home to a tumor in an animal. We anticipate that this high-affinity ligand for $\alpha_v\beta_6$ will find clinical use as a diagnostic and therapeutic reagent. [Mol Cancer Ther 2009;8(5):1239–49]

Introduction

Peptides that recognize cancer cells with high affinity and specificity have promise as reagents for tumor-specific delivery of chemotherapeutics and molecular imaging agents. Phage display has proven a powerful method for the discovery of peptides that bind to cancer cells but not their nonmalignant counterparts. Purified tumor-associated biomarkers, cells in culture, and tumors in animals have been used as bait to identify cancer-binding peptides. However, when these isolated peptides are removed from the phage scaffold and used as free monomeric peptides, their binding affinities are often too weak to be clinically useful as delivery or diagnostic reagents.

We previously identified several 20-amino-acid peptides from a phage-displayed peptide library that bind to different human non–small cell lung cancer cell lines (1). One peptide, named H2009.1, binds to the integrin $\alpha_v\beta_6$ and does not bind other more widely expressed RGD-binding integrins (2). This integrin is overexpressed in many epithelial-derived carcinomas (3–10) but is not found in normal primate tissues (11). The expression of this integrin is correlated with cellular behaviors that are typical of more aggressive tumors (12, 13). Furthermore, $\alpha_v\beta_6$ expression increases during the epithelial-mesenchymal transition, the process in which cells lose their epithelial phenotypes to become motile, implicating a role in metastasis (10). Integrin $\alpha_v\beta_6$ is a biomarker for poor prognosis in several human cancers, including lung, colorectal, and cervical cancers (2, 9, 10). We have shown that the integrin is widely expressed in early-stage non–small cell lung cancer and its expression increases in a stepwise manner with grade (2). In sum, this integrin is emerging as an important target for anticancer therapies. As such, further development of this $\alpha_v\beta_6$-targeting ligand is warranted.

Branched lysine cores provide scaffolds for the synthesis of multimeric peptide dendrimers, often referred to as multiple antigen peptides (14, 15). Tetramerization of the H2009.1 peptide on this trilysine dendrimeric core results in higher affinity for its cellular target than the corresponding monomer. Previous syntheses of the tetrameric H2009.1 peptide were achieved by stepwise solid-phase Fmoc synthesis on a trilysine core (1, 16). Due to the macromolecular structure and complexity, unambiguous synthesis of tetrameric peptides on a trilysine core is difficult. Separation of the desired molecule from the mélange of closely related truncated and deletion products that arise during the synthesis is challenging (15). In addition, the purified products, despite the appearance of being homogeneous by high-performance liquid chromatography (HPLC) analysis, are often heterogeneous, being contaminated with numerous coeluting sequences. Segment condensation has been used to generate tetrameric peptides but current methods have limitations in their use for tumor targeting (15). For these reasons, the utility of these branched peptides is limited in the clinical setting.

To facilitate the use of this $\alpha_v\beta_6$-binding peptide, we report here a facile convergent strategy for multimeric peptide synthesis based on the chemoselective reaction of a thiol to

Received 12/3/08; revised 2/6/09; accepted 2/24/09; published OnlineFirst 5/12/09.

Grant support: NIH grant 1RO1CA106646 and the Welch Foundation (I1622).

The costs of publication of this article were defrayed in part by the payment of page charges. This article must therefore be hereby marked *advertisement* in accordance with 18 U.S.C. Section 1734 solely to indicate this fact.

Requests for reprints: Kathlynn C. Brown, University of Texas Southwestern Medical Center, 5323 Harry Hines Boulevard, Dallas, TX 75390-9185. Phone: 214-645-6348; Fax: 214-648-4156. E-mail: Kathlynn.Brown@UTSouthwestern.edu

doi:10.1158/1535-7163.MCT-08-1098

Published OnlineFirst May 12, 2009; DOI: 10.1158/1535-7163.MCT-08-1098

an activated double bond of a maleimido group. We have optimized the H2009.1 peptide on the trilysine scaffold, reducing its size by half while improving the affinity 10-fold. The affinity of the optimized H2009.1 peptide for its target cell rivals the affinity of more commonly used antibody-targeting reagents.

Experimental Procedures

Peptide Synthesis

Monomeric peptide synthesis was performed on a Symphony Synthesizer (Rainin Instruments, Protein Technologies, Inc.) by Fmoc solid-phase peptide synthesis on a Rink Amide AM resin (substitution level 0.71 mmol/g). Details are available in the Supplementary Data.[3]

Synthesis of Maleimido-Activated Cores

The maleimido tetrameric cores were synthesized on $Fmoc_4$-Lys_2-Lys-β-Ala-CLEAR Acid Resin, $Fmoc_4$-Lys_2-Lys-Lys(Biotin-PEG)-β-Ala-CLEAR Acid Resin, and $Fmoc_4$-Lys_2-Lys-Cys(Acm)-β-Ala-CLEAR Acid Resin, respectively (substitution level 0.21 mmol/g, Peptides International). The maleimido trimeric core was synthesized on Fmoc-β-Ala-CLEAR Acid Resin (substitution level 0.52 mmol/g). Fmoc-Lys(Mtt)-OH was coupled at a 5-fold excess using HBTU, HOBt, and NMM coupling (45 min). Piperidine in DMF (20%) was used to remove NH_2-terminal Fmoc protecting groups. Fmoc-Lys(Fmoc)-OH was coupled in the same manner. The 4-methytrityl (Mtt) protecting group was removed by treatment with 1% trifluoroacetic acid in dichloromethane for 2 min, five times (17). Maleimidopropionic acid was coupled to all lysine cores in 5-fold excess using HBTU, HOBt, and NMM (24 h, room temperature). The activated core was cleaved from the resin using a trifluoroacetic acid/triisopropylsilane/H_2O cocktail, precipitated in cold diethyl ether, and purified by reverse-phase HPLC. Characterization is reported in the Supplementary Data.[3]

Multimeric Peptide Synthesis

The peptide (8 μmol) and appropriate maleimide-activated core (1 μmol) were dissolved in 1.5 mL of Ar-purged PBS (pH 7.4) containing 0.01 mol/L EDTA. The reaction mixture was stirred at room temperature for 2 h. Details are included in the Supplementary Data.[3]

Peptide Blocking Experiments

The ability of the peptides to block their cognate phage was determined as described (1, 18).

Labeling of the Peptide with Alexa Fluor 488

The acetamidomethyl group on the cysteine was removed according to published procedures (19). A solution of 0.015 μmol H2009.1 tetrameric-SH peptide was prepared in 500 μL of Ar-purged 1× PBS/0.01 mol/L EDTA. A solution of 0.15 μmol Alexa Fluor 488 C_5-maleimide dye ($C_{30}H_{25}N_4NaO_{12}S_2$, Invitrogen Corporation) in 50 μL PBS was added. The mixture was stirred at room temperature for 12 h before adding 0.75 μmol mercaptoethanol to consume excess thiol-reactive dye. The products were purified by HPLC and analyzed by matrix-assisted laser desorption/ionization mass spectrometry (Supplementary Data).[3]

Cellular Uptake of the Peptide

The biotin-labeled tetrameric peptide (4,000 nmol/L) was incubated with Streptavidin-Qdot 605 made in-house (SAQdot605, 200 nmol/L) for 2 h at room temperature. The peptide-SAQdot605 conjugate solution were diluted with PBS^+/0.1% bovine serum albumin to a final Qdot concentration of 20 nmol/L before overlaying onto cells as described (18). Similarly, H2009 cells were incubated for 10 min at 37°C with 1 μmol/L peptide-Alexa Fluor 488 conjugate. β_6 was observed using anti-β_6 antibodies (2). Images were captured on a Leica TCS SP5 confocal microscope at 400× magnification with 7× optical zoom.

Flow Cytometric Analysis

Cells were grown to 80% to 90% confluency in a 12-well plate (3.87 cm^2). Cells were treated with serum-free RPMI (2 h, 37°C) to clear the cellular receptors. Peptide-dye solutions in PBS^+ supplemented with chloroquine and protease inhibitor cocktail were placed on the cells (1 mL/well, 1 h at 37°C). Cells were washed four times with PBS^+, released from the wells by incubation in Enzyme-Free Cell Dissociation Buffer (10 min, room temperature), and analyzed on a Quanta Flow Cytometer (Beckman Coulter).

Peptide Binding to Tumor Samples

One million cells were inoculated s.c. on the flanks of immunodeficient mice. Tumors were grown for 19 d. Mice were perfused with PBS followed by the formalin fixative. Tumors were processed for paraffin block sectioning. One slide from each tumor was stained with H&E whereas serial sections were stained with peptide-labeled Qdots(605 nm) or unlabeled Qdots. For Qdot staining, slides were treated with EZ-DeWax (BioGenex) per manufacturer's protocol. Slides were incubated in 300 mL of 10 mmol/L sodium citrate-citric acid buffer (pH 6.0), 90°C, for 10 min, then allowed to cool to room temperature. Slides were rinsed with TBS [100 mmol/L Tris-HCl (pH 7.4), 138 mmol/L NaCl, 17 mmol/L KCl] and blocked in TBS supplemented with 1% goat serum and 1% bovine serum albumin. H2009.1-Qdots were prepared as detailed above. Tumor sections were incubated with peptide-labeled or control Qdots suspended in PBS + 0.1% bovine serum albumin for 30 min at room temperature. Slides were washed four times in TBS + 0.1% bovine serum albumin. Vectashield containing Hoechst dye was applied to the slide before imaging.

Preparation of ^{111}In-Labeled Peptides

The maleimide precursor (4,10-Bis-carboxymethyl-7-{[2-(2,5-dioxo-2,5-dihydro-pyrrol-1-yl)-ethylcarbamoyl]-methyl}-1,4,7,10tetraaza-cyclododec-1-yl)-acetic acid; Macrocyclics) was reacted with the thiol of the cysteine (molar ratio: 5:1, 2 h, room temperature) in 10 mmol/L PBS containing 10 mmol/L EDTA. The 1,4,7,10-tetraazacyclododecane-1,4,7,10-tetraacetic acid (DOTA)–conjugated peptides were separated by Waters XTera C_{18} HPLC system (Waters) and confirmed through mass spectrometry. ^{111}In was loaded

[3] Supplementary material for this article is available at Molecular Cancer Therapeutics Online (http://mct.aacrjournals.org/).

Published OnlineFirst May 12, 2009; DOI: 10.1158/1535-7163.MCT-08-1098

by a standard protocol. Details are included in the Supplementary Data.[3]

In vitro Serum Stability

To 100 μL of rat serum, 10 μL of ^{111}In-labeled peptide solutions were added. The solution was incubated at 37°C. After 1 and 4 h postaddition, an aliquot of 30 μL was mixed with 100 μL of ethanol to precipitate serum proteins. The mixture was centrifuged at 14,000 rpm for 10 min. The pellets were resuspended with 80% ethanol, followed by centrifugation. The pellets and the pooled supernatants were counted by a γ-counter. The ^{111}In-labeled peptides in the supernatant were identified by radio-HPLC. The serum stability of ^{111}In-labeled peptides is presented as the product of the HPLC-determined radiochemical purity of the labeled peptide in the supernatant and the percentage of the pooled supernatant γ counts of the total counts.

In vivo Biodistribution of H2009 Tumor-Bearing Mice

Tumors were established by s.c. injection of a cell suspension (1×10^6 cell) as described and grown for 16 d, resulting in tumors of 60 to 200 mg. Each mouse received 5 μCi of the ^{111}In-labeled peptides i.v. ($n = 4$). Mice were sacrificed 4 h postinjection. The percentage of injected dose per gram was determined for the tumor, blood, and muscle. The animal protocols were approved by the University of Texas Southwestern Medical Center's Institutional Animal Care and Use Committee.

Results

Development of a Simple Convergent Strategy for Synthesis of Tetrameric H2009.1 Peptide

As an alternative to the reported synthesis of tetrameric peptides on trilysine cores, we used a synthetic route that takes advantage of the chemoselective reaction of a cysteine with a maleimide (Fig. 1). Although this approach has been suggested (15), its use has not been reported for the synthesis of these dendrimers. The activated N-maleimido trilysine core was synthesized by the reaction of 3-maleimidopropionic acid with Lys_2-Lys-β-Ala on a CLEAR Acid Resin solid support. The fully deprotected H2009.1 peptide containing a unique cysteine (NH_2-RGDLATLRQ-LAQEDGVVGVR-PEG_{11}C-$CONH_2$) was synthesized in 63% yield. A polyethylene glycol (PEG) linker was incorporated to increase solubility of the peptides in aqueous solution and prevent possible compaction of the peptides on the trilysine core. The reaction of the cysteinyl peptide with the activated trilysine core on the solid support was unsuccessful under a variety of conditions, including a 2.5-fold molar excess of peptide, reaction times up to 48 hours, and use of organic cosolvents. However, the removal of the N-alkyl maleimide-activated trilysine from the solid support followed by a solution phase coupling of the peptide in aqueous buffer for 2 hours at room temperature resulted in production of four-branch peptide in 85% yield. The tetrameric peptide was purified from the small amounts of contaminating one-, two-, and three-branched peptides by reverse-phase HPLC. The resultant tetrameric peptide was >95% pure based on analytic HPLC analysis.

Tetrameric H2009.1 Synthesized by the Convergent Strategy Is Functional as a Cell Binding Reagent

There are structural differences in the linker of the peptides obtained by linear synthesis and the convergent synthesis. Although distant from the cell binding peptide, this may affect cell binding. As this peptide was initially selected as a bacteriophage clone through biopanning on the human lung adenocarcinoma cell line H2009 (1), the ability of this peptide to block binding of its cognate phage on H2009 cells was assessed. This assay has the advantage in that it can be used in cases in which purified membrane proteins are unavailable or when the cellular target of the peptide ligand is unknown. Additionally, it screens for binding in a more relevant cellular context and can be used when the peptides mediate cellular uptake in addition to cell surface binding. By this assay, the peptides perform identically over a 10,000-fold concentration range and

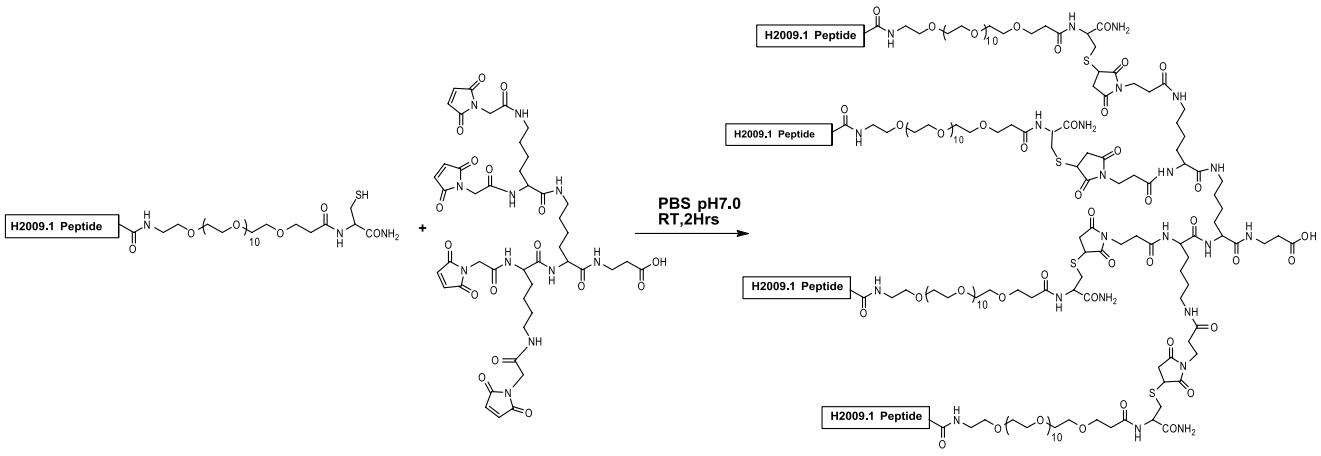

Figure 1. Synthetic scheme for the convergent synthesis of tetrameric peptides. H2009.1 peptide sequence: RGDLATLRQLAQEDGVVGVR, RGDLATLRQL, or RGDLATL.

Published OnlineFirst May 12, 2009; DOI: 10.1158/1535-7163.MCT-08-1098

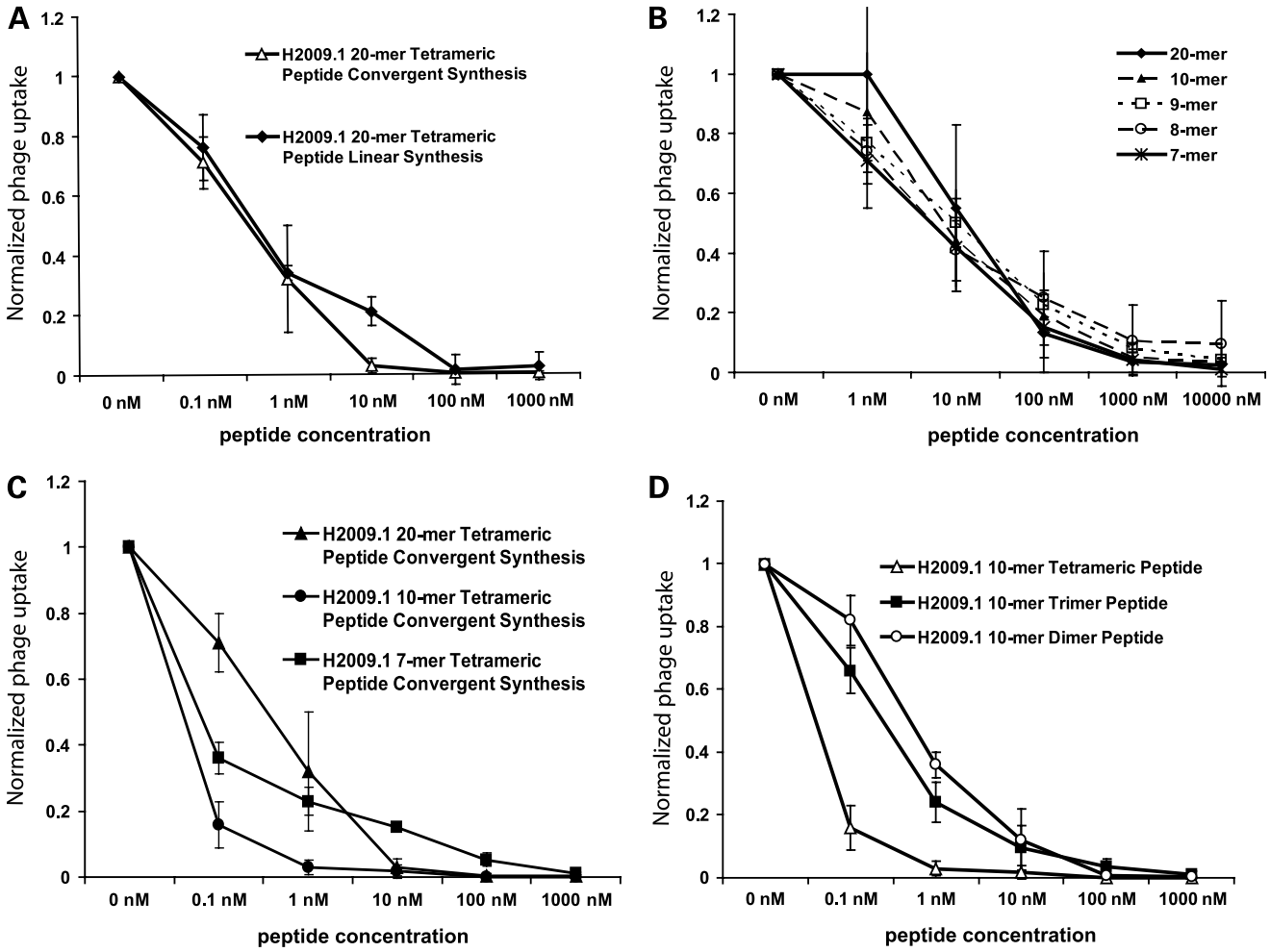

Figure 2. Inhibition of bacteriophage uptake by different peptide scaffolds synthesized by the convergent strategy. The normalized phage uptake is defined as the ratio of output phage to input phage in the presence of peptide normalized to the output/input ratio of phage with no peptide added (1, 18). The number of input phage particles was held constant. *Error bars,* SE measurement of a minimum of three replicates. **A,** comparison of the inhibition of bacteriophage uptake by the H2009.1 20-mer peptides prepared by either convergent or linear synthesis. Synthesis of the peptide by linear synthesis and its ability to block phage uptake has been previously reported (16). **B,** the truncated 10-mer peptide blocks uptake of the H2009.1 phage clone as efficiently as the full-length 20-mer H2009.1 peptide. Single amino acid deletions from the carboxy terminus reveal that the minimal binding domain is a seven-amino-acid peptide. **C,** comparison of effect of peptide length on binding when placed on the trilysine core. **D,** evaluation of the effect of valency on peptide affinity.

display half-maximal binding in the 0.6 to 0.8 nmol/L range (Fig. 2A).

Identification of the Minimal Peptide Binding Domain

The ease of synthesis allows for optimization of the peptides by chemical approaches as opposed to repanning mutagenic phage-displayed peptide libraries. This has the benefit in that optimization occurs on the format in which the peptides will later be used. The H2009.1 20-mer peptide was selected from a random library of 20-amino-acid peptides. Alanine scanning was done to address which residues are critical for binding of the peptide to its receptor. A set of four monomeric peptides was synthesized in which amino acids 1 to 5, 6 to 10, 11 to 15, or 16 to 20 were replaced by alanines. Changing amino acids 1 to 5 or 6 to 10 to alanine inactivates the ability of the peptide to block phage uptake (Supplementary Data).[3] The last 10 amino acids can be changed to alanine with no loss of binding affinity of the peptide for H2009 cells. Consistent with this observation, the NH_2 terminus contains a known binding motif for $\alpha_v\beta_6$ (2, 20). As confirmation, the H2009.1 10-mer peptide possessing the NH_2-terminal 10 residues of parent peptide (sequence: RGDLATLRQL-$CONH_2$) was synthesized. As expected, the 10-mer peptide behaves the same as the parental 20-mer peptide (Fig. 2B). Of note, the carboxy-terminal amide is important for binding as the corresponding peptide, RGDLATLRQL-COOH, shows significantly reduced affinity (data not shown). Amino acid deletions were made from the carboxylterminus of the 10-mer peptide. The peptide retains full activity as a 7-mer. Truncations past this point result in loss of peptide binding.

Published OnlineFirst May 12, 2009; DOI: 10.1158/1535-7163.MCT-08-1098

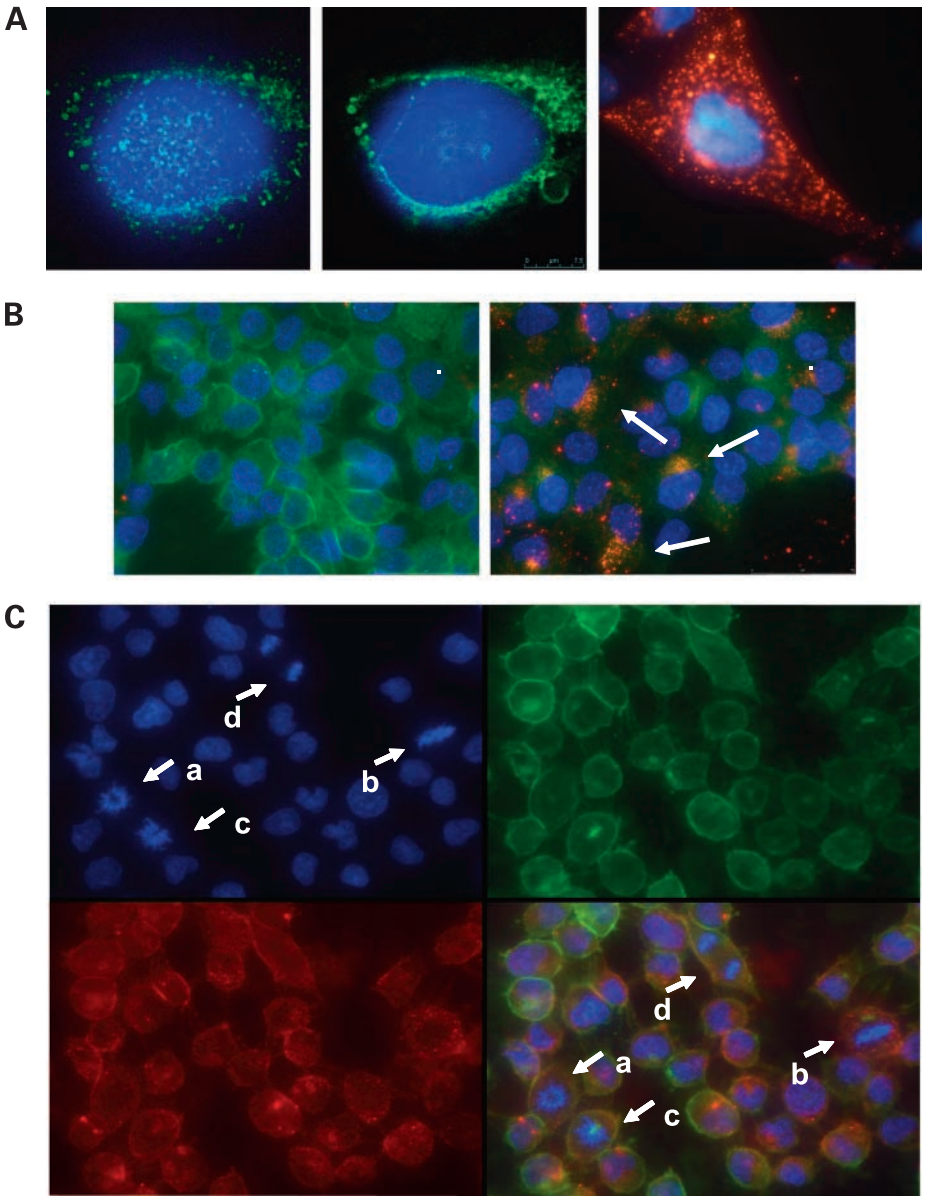

Figure 3. The tetrameric 10-mer H2009.1 peptide mediates cellular uptake. **A,** H2009 cells were incubated for 10 min at 37°C with 1 μmol/L H2009.1 10-mer tetramer-Alexa Fluor 488 conjugate. Images were captured on a Leica TCS SP5 confocal microscope at 400× magnification with 7× optical zoom. Images are presented as an overlay series of 18 frames from the Z-stack acquisition (*left*). A single z-series slice from the image obtained in frame to the left is shown (*middle*). The H2009.1 10-mer tetrameric peptide mediates cellular uptake of Qdots in H2009 cells (*right*). The peptide was conjugated to the Qdot through a streptavidin-biotin interaction. Cells were incubated with 20 nmol/L of the SAQdot605-conjugated tetrameric H2009.1 peptide. In all panels, similar data were collected from distinct areas of the slide. **B,** H2009.1 cells were treated with H2009.1-Qdot conjugate (*right*) or H1299.2-Qdot conjugate (*left*). After incubation, the cells were fixed, permeabilized, and stained for β_6 (*green*). Within the 10-min incubation time, the H2009.1-Qdot conjugate and the β_6 integrin are internalized. Colocalization of the H2009.1-Qdot conjugate and β_6 is indicated by the yellow color and pointed out by the arrows for several cells. H2009 cells do not mediate uptake of the H1299.2-Qdot conjugate (*left*). Additionally, the β_6 integrin remains on the cell surface. **C,** uptake of peptide-conjugated Qdots is independent of cell cycle progression. Cells were cultured overnight in eight-well chamber slides before incubation with 10 nmol/L Qdot-H2009.1 peptide conjugate for 10 min at 37°C. Wells were washed and fixed in PBS-buffered formalin as detailed in Experimental Procedures. Cellular DNA was stained with 4′,6-diamidino-2-phenylindole (*top left*) and the cell membrane was stained with wheat germ agglutinin-Alexa Fluor 488 (*top right*). *Bottom left,* Qdot uptake; *bottom right,* an overlay of the three images. *Arrows,* cells captured during mitosis: *a,* prophase; *b,* metaphase; *c,* early anaphase; and *d,* late telophase/cytokinesis.

We anticipated that tetramerization of the shorter H2009.1 peptides would increase its affinity for H2009 cells in the same manner as observed for the 20-mer peptide. The H2009.1 10-mer and 7-mer tetrameric peptides were synthesized in 91% and 89% yield, respectively. The H2009.1 10-mer and 7-mer tetrameric peptides inhibit phage uptake by >97% at concentrations above 100 nmol/L on H2009 cell (Fig. 2C). Similar results are observed for H2009.1 20-mer tetrameric peptide

Published OnlineFirst May 12, 2009; DOI: 10.1158/1535-7163.MCT-08-1098

at the same concentration. Surprisingly, at 1 nmol/L, the H2009.1 10-mer and 7-mer tetrameric peptides inhibit phage uptake 10.8- and 1.4-fold more than H2009.1 20-mer tetrameric peptide, respectively; the monomeric peptides have uniform potency at this concentration. Impressively, the half-maximal binding is in the 40 to 60 pmol/L for the 10-mer tetrameric peptide and 80 to 100 pmol/L for the 7-mer. These results indicate that the carboxy-terminal 10-amino-acid residues contribute negatively to the binding affinity in the context of the four-branched peptides. The reason for this is unknown. It is possible that the orientation of the peptide branches on the 10-mer is better suited for receptor binding on the cell surface. Alternatively, the last 10 amino acids do not contribute to the enthalpy of binding but their entropy may decrease in the process of binding to the cellular receptor, resulting in a decreased binding affinity (21). Nonetheless, our results show that the tetrameric 10-mer has enhanced cellular binding. Furthermore, the peptidic targeting reagent is surpassing the affinities observed with more commonly used antibody-targeting reagents (22).

Identification of the Optimal Valency

In attempt to reduce the peptide size, the minimal required valency was explored. The H2009.1 10-mer dimeric and trimeric peptides were synthesized by the convergent strategy. The dimeric lysine core was made on Rink Amide AM resin using Fmoc solid phase peptide synthesis strategy with a yield of 93%. The maleimido trimeric core was synthesized using a chemically orthogonal–protected lysine (Mtt-protected C-amino group of the first lysine). Coupling of the peptides to these scaffolds was done in the same manner as that used for the tetrameric cores.

The dimeric and trimeric peptides display higher phage blocking ability than the corresponding monomeric peptide, corroborating the superiority of peptide multimerization in increasing the affinity of the peptide for its cellular target (Fig. 2D). However, the tetramer construct obstructs phage uptake at lower concentrations when compared with the dimeric and trimer peptide, suggesting that the optimal scaffold is the tetramer for this group of peptides. Higher valencies were not tested.

Chemical Tags Can Be Incorporated into the Trilysine Core

The sulfhydryl group of a cysteine is frequently used for attachment of peptides to drugs, drug carriers, or imaging agents (16, 23). Thus, the synthetic strategy used here would have greater utility if it is compatible with the protection/deprotection of other chemically orthogonal thiol-protecting groups. To determine if the four-branch peptide could be synthesized and subsequently deprotected to reveal a free thiol, the H2009.1 10-mer tetrameric peptide was coupled to a maleimide trilysine core containing an acetamidomethyl-protected cysteine before the branch point. The acetamidomethyl group was removed by treatment with Ag(I) (98% yield; ref. 19). No loss of the peptide branches was observed (Supplementary Data).[3] The peptide can be labeled by reaction of Alexa Fluor 488 C_5-maleimide dye, confirming the integrity of the revealed thiol moiety. Thus, the thiol ether bond formed between the peptide and the lysine core is chemically compatible with removal of the acetamidomethyl group from a strategically placed cysteine.

Another useful chemical moiety is biotin as many streptavidin reagents exist for biological applications. Therefore, we synthesized an activated trilysine core that contained a biotinylated lysine before the branch point using a $Fmoc_4$-Lys_2-Lys-Lys(Biotin-PEG)-β-Ala-CLEAR Acid Resin. The biotin was fully compatible with the downstream chemistry and was functional in binding streptavidin.

The Optimized Peptide Can Mediate Cellular Uptake

For the smaller peptide to be of utility as a drug delivery reagent, it must mediate cellular uptake specifically in $\alpha_v\beta_6$-positive cells. To address this, the Alexa Fluor 488–labeled H2009.1 10-mer tetrameric peptide was incubated with H2009 cells. The cellular localization of the peptide was determined by confocal microscopy. The peptide-dye conjugate is internalized into the cells (Fig. 3A; Supplementary Data).[3] As confirmation, the biotinylated peptide was conjugated to a streptavidin-coated fluorescent quantum dot (SAQdot605) and incubated with H2009 cells. Punctate staining is observed in the cytoplasm by fluorescent microscopy, indicative of cellular uptake of the nanoparticle through an endocytosis process (Fig. 3A). A Z-stacked series obtained by confocal microscopy confirms the internalization of the particle (Supplementary Data).[3] Additionally, the peptide mediates internalization of the β_6 integrin. The peptide Qdot complex colocalizes with $\alpha_v\beta_6$ within the H2009 cells, indicative that the H2009.1 10-mer tetrameric peptide is mediating uptake through $\alpha_v\beta_6$-mediated endocytosis (Fig. 3B). No uptake is observed for unconjugated Qdots or when a scrambled H2009.1 peptide (DALRLQGTLR) is conjugated to Qdots. Additionally, no uptake is seen when another peptide with no affinity for $\alpha_v\beta_6$ is used (H1299.2, sequence: YAAWPASGAWTGTAPC-SAGT) (Fig. 3; Supplementary Data).[3] When H2009 cells are treated with the H1299.2-Qdot conjugate, β_6 remains localized on the cell surface, demonstrating that the internalization of β_6 is triggered by binding of the H2009.1 10-mer tetrameric peptide. The peptide retains its cell specificity as well; no uptake of the H2009.1 10-mer tetrameric peptide is observed in a cell line with insignificant expression of $\alpha_v\beta_6$ (Supplementary Data).[3]

Peptide-Qdot uptake is observed in cells that are in varying stages of the cell cycle. As seen in Fig. 3C, the peptide-Qdot conjugate is observed in cells in prophase, metaphase, early anaphase, and late telophase/cytokinesis. As the incubation time is only 10 minutes, this suggests that cellular uptake of the peptide by $\alpha_v\beta_6$ can occur at any point along the cell cycle. Thus, cells do not need to be synchronized to use this reagent *in vitro*, and *in vivo* targeting will be cell cycle independent. Furthermore, it appears that the peptide-Qdots are being retained during cell division. This is consistent with other reports that show the utility of Qdots to track cells through multiple cell divisions (24).

The Peptide Can Be Employed in Diagnostic Applications

Antibodies are routinely used to obtain molecular information about tumors. Clinical samples are most commonly

Published OnlineFirst May 12, 2009; DOI: 10.1158/1535-7163.MCT-08-1098

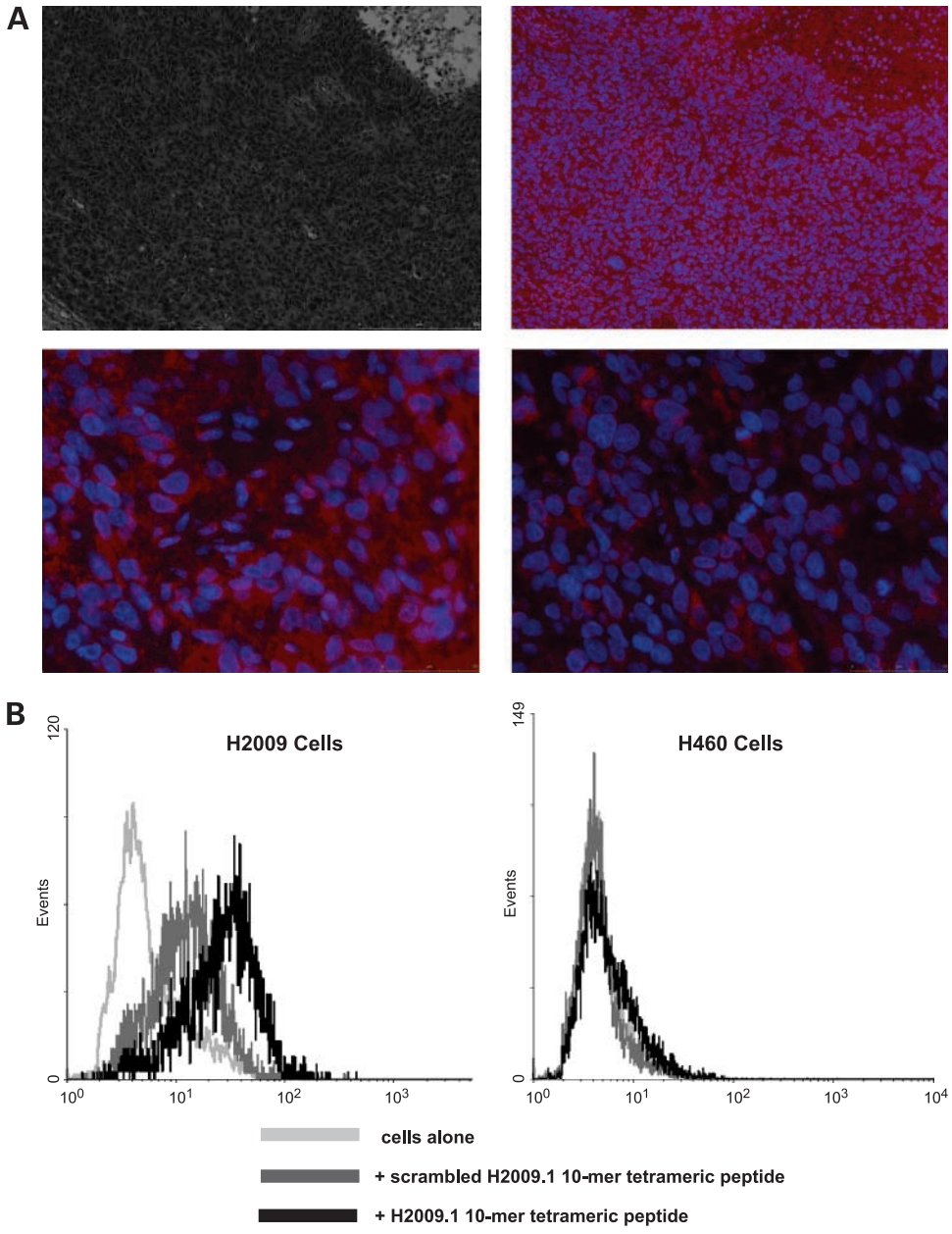

Figure 4. The H2009.1 10-mer tetrameric peptide can be used in diagnostic formats. **A,** formalin-fixed, paraffin-embedded tumor sections were stained with H&E (*top left*) or H2009.1 10-mer peptide-labeled Qdots (*top right* and *bottom left*) or Qdots with no peptide (*bottom right*). *Bottom left* (400× magnification), peptide-labeled Qdot staining (*red*) is associated with intact tumor cells as indicated by the staining of nuclei (*blue*), whereas unlabeled Qdots exhibit minimal cellular staining. At 100× magnification (*top right*), the labeled Qdot staining appears uniform throughout the tumor. Similar results were observed with independently prepared tumor specimens. **B,** the H2009.1 10-mer tetrameric peptide can be used as a flow cytometry reagent to bind to $\alpha_v\beta_6$-positive cells. Cells ($\alpha_v\beta_6$-positive H2009 cells and $\alpha_v\beta_6$-negative H460 cells; ref. 2) were incubated for 1 h with H2009.1 10-mer peptide-Alexa Fluor 488 conjugate or scrambled peptide-dye conjugate, washed, and evaluated for peptide-dye uptake by flow cytometry. Cells were gated by cell volume and side scatter to remove cell fragments and debris from analysis. A total of 10,000 events were evaluated for fluorescence in channel 1 (excitation at 488 nm, emission at 500–550 nm). The data shown were obtained at 10 nmol/L peptide-dye conjugate concentration.

presented as formalin-fixed paraffin samples, not fresh tumors. The utility of the H2009.1 peptide for clinical diagnosis would be expanded if it is bound to fixed tumor samples. To address this, H2009 tumors grown s.c. in a severe combined immunodeficiency mouse were fixed in paraformaldehyde and embedded in paraffin. As seen in Fig. 4, the peptide-Qdot conjugate can bind a fixed non–small cell lung cancer $\alpha_v\beta_6$-positive tumor sample. Less binding is observed when Qdots alone are used. Thus, the peptide can serve as a complementary reagent to $\alpha_v\beta_6$ antibodies. As peptide-Qdot conjugates can be multiplexed by using different peptide-Qdot pairs, this opens the possibility of assaying for multiple biomarkers on a single sample.

Additionally, flow cytometry is used to determine the expression levels of biomarkers as an aid for diagnosis (25). Although flow cytometry has been primarily used for nonadherent cells, there is increasing interest in using it for the detection of circulating cancer cells that have been shed from the solid tumor. As $\alpha_v\beta_6$ is overexpressed on many epithelial-derived cancers, this peptide may be of utility to detect $\alpha_v\beta_6$-positive cells in the bloodstream. The Alexa Fluor 488–labeled H2009.1 10-mer tetrameric peptide was incubated with H2009 cells. As shown in Fig. 4B, the peptide is functional as a flow cytometry reagent to recognize $\alpha_v\beta_6$-expressing cells, such as H2009. Cells treated with labeled H2009.1 10-mer tetrameric peptide have mean

Published OnlineFirst May 12, 2009; DOI: 10.1158/1535-7163.MCT-08-1098

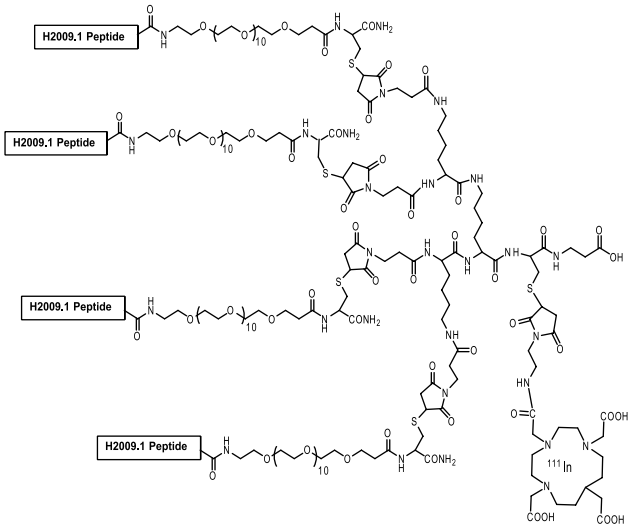

Figure 5. Structure of the DOTA-labeled tetrameric peptide.

fluorescence intensity that is 2-fold greater than when the scrambled peptide is used. H460 cells that do not express significant amounts of $\alpha_v\beta_6$ (2) exhibit minimal binding to the H2009.1 10-mer tetrameric peptide (Fig. 4B). The results suggest that this peptide may have utility as a detection or capture reagent of $\alpha_v\beta_6$-expressing cells.

The Peptide Is Stable in Sera

To be of utility *in vivo*, the peptide must remain intact in serum long enough to home to its cellular target. Historically, serum stability has often been cited as a drawback of peptide therapeutics, although PEGylation and glycosylation can increase the peptide half-life *in vivo* (26). Peptides synthesized on trilysine cores are more serum stable than their monomeric counterparts (27, 28). However, we have introduced a thiol ether bond into the peptide that might have different serum stability than the native amide.

To evaluate the serum stability of peptide conjugates *in vitro*, we radiolabeled the monomeric H2009.1 10-mer, H2009.1 10-mer tetrameric peptide synthesized by convergent strategy, and the corresponding tetramer synthesized by linear Fmoc SPPS. The peptides were modified by placing a DOTA chelator towards the COOH terminus of the peptide and subsequently loaded with ^{111}In (Fig. 5). The ^{111}In-labeled peptides were incubated with rat serum at 37°C. After 1 and 4 h, an aliquot was removed and the serum proteins were precipitated in ethanol. The supernatants were counted by a γ-counter and the amount of full-length ^{111}In-labeled peptides were identified by radio-HPLC. The results are shown in Table 1. As expected from previous reports, the tetrameric peptides are more stable than the monomeric peptide (27, 28). At 4 hours, a significant fraction of the peptide remains intact for all three peptides. At this time point, similar amounts of tetrameric peptides remain intact regardless of the synthetic route, indicating the thioether bond to be suitable for *in vivo* applications. This suggests that the peptides will have the serum stability necessary for *in vivo* applications.

This method measures total radiochemical stability, such that both proteolysis and loss of the radio metal from the DOTA moiety will contribute to the overall loss of the HPLC signal. However, this method is more sensitive and quantitative than standard HPLC methods. Additionally, it measures the total stability of a peptide conjugate that can be used for single-photon emission computed tomography or positron emission tomography imaging. The resultant peptides after treatment in sera were not characterized. Additionally, these studies do not address the clearance rate of the peptides in an animal.

The Peptide Can Reach Its Tumor Target in an Animal Model

To determine if the peptide could reach its target *in vivo* and might possibly serve as a molecular imaging reagent, the ^{111}In-labeled peptides were injected i.v. into tumor-bearing severe combined immunodeficiency mice. One and 4 hours after injection, the animals were sacrificed and the tumors were collected, weighed, and counted by a gamma counter. The percentage of injected dose per gram was determined for the tumor, blood, and muscle. At 1 hour, the H2009 tumor retains 3.15 ± 0.47 of the total dose per gram (%ID/g) of tissue and the tumor to blood ratio is 1.37 ± 0.14. By 4 hours, the tumor accumulates 2.25 ± 0.47% D/g of tissue and the tumor to blood ratio is 2.43 ± 0.14. By comparison, the corresponding scrambled sequence peptide had only 0.59 ± 0.30% of the total dose per gram of tissue retained in the tumor at 4 hours (tumor to blood ratio of 0.44 ± 0.22). Substantially less accumulation of peptide in the tumor is observed when a non–$\alpha_v\beta_6$-expressing tumor is implanted in the animal ($\alpha_v\beta_6$-negative H460 lung cancer cells, at 1 hour: tumor accumulation of 0.96 ± 0.16%ID/g, tumor to blood ratio of 0.81 ± 0.14; at 4 hours: tumor accumulation of 0.84 ± 0.11%ID/g, tumor to blood ratio of 2.0). The tumor to muscle ratio for the H2009 tumors is 3.92 ± 0.35%ID/g and 4.43 ± 0.03%ID/g at 1 and 4 hours, respectively. By comparison, the tumor to muscle ratio for the H460 tumors is 0.80 ± 0.15%ID/g (1 hour) and 1.54 ± 0.19%ID/g (4 hour). In sum, these data show the H2009.1 peptides have the stability, specificity, and affinity to target $\alpha_v\beta_6$-positive tumors in animal models. The tumor to blood ratio is favorable for the development of the peptide as a single-photon emission computed tomography and positron emission tomography imaging agent. A full pharmacokinetic profile must be done to fully

Table 1. Serum stability of H2009.1 peptides

	1 h	4 h
	% Intact	% Intact
H2009.1 10-mer-PEG11-DOTA	60	46
H2009.1 10-mer-tetramer (convergent)	76	69
H2009.1 10-mer-tetramer (linear)	73	63

Published OnlineFirst May 12, 2009; DOI: 10.1158/1535-7163.MCT-08-1098

understand the fate of the peptide in other organs and the $\alpha_v\beta_6$ expression profile in a mouse (11, 29).

Discussion

The integrin $\alpha_v\beta_6$ is increasingly being considered as a candidate for targeted therapies for epithelial-derived cancers. As such, high-affinity and high-specificity ligands for this integrin target are needed. Toward this goal, we have identified a peptide that binds specifically to $\alpha_v\beta_6$ within the context of the cell membrane. Our advancements to the overall synthetic route and optimal presentation expand the possible clinical uses of this targeting ligand. Furthermore, our peptide is functional in multiple applications.

The ease of the synthetic route allowed us to determine the optimal length and valency of a specific peptide, H2009.1. Through systematic mutations and truncations, the peptide was reduced from 20 amino acids to 7. Consistent with our results, the $\alpha_v\beta_6$ is an RGD binding integrin and native ligands for $\alpha_v\beta_6$ typically have an RGDLXXL/I motif (20, 30). The decrease in the size of the peptide speeds the synthesis and reduces the cost of the targeting moiety. It also has the added benefit of reducing the potential of untoward proteolysis and immune responses to the peptide. Experiments to determine the optimal amino acids in positions 5 and 6 of the peptide are under way in our laboratory. Although we could reduce the size of the peptide chain, the tetrameric peptide has a higher affinity than the corresponding dimer or trimer. However, for *in vivo* delivery, there is a fine balance between affinity, stability, nonspecific uptake, and clearance. As such, the lower valency peptides may be superior for some applications.

The emergence of $\alpha_v\beta_6$ as an important therapeutic target for epithelial-derived cancers has led to the design of ligands for this cell surface receptor. Small-molecule inhibitors (31) and function blocking antibodies are being developed against this target (32, 33). Although promising, peptides combine the high specificity and affinity of antibodies with the small size and synthetic availability of small molecules. DiCara and colleagues (34) have recently characterized three 20-mer peptides for $\alpha_v\beta_6$ binding. The peptides are derived from two of the $\alpha_v\beta_6$ naturally occurring ligands, foot and mouth disease virus, and the latency-associated peptide of transforming growth factor-β (35, 36). The peptides A20FMDV1 (sequence: YTASARGDLAHLTTTHARHL), A20FMDV2 (sequence: NAVPNLRGDLQCLAQKVART), and A20LAP (GFTTGRRGDLATIHGMNPF) contain the RGDLXXL/I motif and bind $\alpha_v\beta_6$ with affinities in the low nanomolar range. Interestingly, the affinity of the peptides is correlated with the α helicity of the peptides. The conserved leucine or isoleucine at positions Asp+1 and Asp+4 may make important contacts with the integrin at the binding interface, and placing these residues on the same face of the helix increases the affinity. The A20FMDV2 peptide has recently been used as a positron emission imaging reagent for $\alpha_v\beta_6$-positive tumors in a mouse model (37). In contrast to our work, shorter peptides (7–12 amino acids) derived from these sequences had reduced affinity compared with the longer 20-mer peptides.

Of the H2009.1 monomeric peptides, the predicted α-helical propensity of the peptides is 20-mer >10-mer >>7-mer using Agadir secondary structure prediction software (Supplementary Data).[3] Yet, we observe no difference in the binding affinity of these three peptides. Perhaps the H2009.1 peptides may be unstructured as in the case of the A20FMDV1 peptide. Alternatively, the flanking sequences to the RGDLXXL/I motif may play a role in binding that is independent of the secondary structure. Further structural analysis is needed to better understand the structure function relationship of these peptides.

Peptides are particularly appealing ligands for cell targeting. They are easier to chemically manipulate and less costly to produce than currently used antibody reagents. Small peptides can avoid uptake of the reticuloendothelial system, which can be problematic with antibodies. Importantly, peptide libraries can be screened for cell binding. Both one-bead/one-compound and phage-displayed peptide libraries have been used a source for cell binding ligands, and both are amenable to using intact cells (38, 39). This opens up the route to identifying cell-specific peptide ligands without a priori knowledge of the cellular receptor. Due to the need for tumor-specific reagents for chemotherapeutic targeting, cancer cell lines have been used as the bait in many of these selections (40).

Retaining the affinity and activity of peptides selected from phage-displayed libraries has been a challenge in the field. To overcome this, many have used a cyclic peptide library whose conformation is constrained by a disulfide bond. Although useful, peptides with disulfides may present challenges in downstream *in vivo* applications or in the attachment of these peptides to drug carriers. The trilysine scaffold mimics the presentation of the peptides on the pIII protein of the phage in both the valency and the orientation of the displayed peptides. We have found the tetrameric trilysine framework to be a general platform for cell-targeting peptides selected from bacteriophage-displayed peptide libraries (18, 41–43). Peptides on this scaffold retain their cell specificity as well as their ability to mediate cellular internalization when removed from the phage particle.

Bracci et al. (44, 45) first reported the utility of trilysine scaffolds for placing targeting peptides. Surprisingly, multimerization did not increase the affinity of the peptide for its target but increased the serum stability, leading to an increase in efficacy *in vivo*. Recently, they have placed a six-amino-acid neurotensin fragment on a tetrameric trilysine dendrimer; the peptide can deliver an active chemotherapeutic to tumors overexpressing the neurotensin receptor (28). Of note, the peptides used in these experiments were not selected from a phage-displayed library. Additionally, the peptides were optimized on purified protein targets not whole cells. This could account for similar affinities of the monomeric and tetrameric peptides.

Despite the utility of the trilysine scaffold, the synthesis of these multimeric peptides is difficult, especially for longer peptides. The possibility for incomplete coupling for every additional residue along any of the branches results in complicated mixture of compounds. To overcome the problems

involved in linear synthesis, segment condensation has been used. However, the coupling rates in segment condensation are slow and the solubility of protected peptide segments is unpredictable (46). Other methods based on the site-specific ligation of unprotected peptide segments through formation of thioether (47), oxime (48), hydrazone (49), or thiazolidine (50) linkages have been developed. These approaches have met with success; however, the oxime- and hydrazone-derived dendrimers may not be appropriate for tumor targeting due to their potential instability in the acidic tumor environment. Additionally, formation of thiazolidine linkage occurs through an NH_2-terminal cysteine. This orientation is opposite of how the peptides are displayed as a fusion on the phage particle and may not be appropriate for the synthesis of multimeric peptides that require a free amino terminus for activity. Last, the formation of thioethers through reaction of a sulfhydryl with a haloacetyl often requires basic conditions, resulting in the formation of peptide dimer side products as a result of disulfide formation. By comparison, our method allows for tetrameric peptides to be produced in 85% to 95% yield and >95% purity. Of note, the overall synthetic yield of the H2009.1 10-mer tetrameric peptide is 68% after purification, taking into account the yield of the monomeric peptide synthesis and the conjugation yield. By comparison, the same peptide synthesized by the Fmoc linear method has an overall yield of 8% after purification.

This chemistry is not restricted to laboratories with expertise in synthetic peptide chemistry. As such, this approach is useful to all performing phage display selections. We have recently selected a peptide from the commercially available NEB PhD 12-mer phage-displayed peptide library that binds to a squamous cell lung carcinoma. Tetramerization of this peptide by this synthetic route increases its affinity for its target cell type by 200-fold and has a half-maximal binding affinity of 30 pmol/L.[4] The chemistry allows for a variety of chemical moieties to be placed in the peptide in a regiospecific manner, expanding the utility of the peptide. This route will be of utility to the many laboratories performing phage display selections, many of which are focused on isolation of tumor-targeting peptides (40).

This simple synthesis of tetrameric peptides widely expands the use of ligands isolated from phage-displayed peptide libraries. This method has produced a peptide that binds specifically to the integrin $\alpha_v\beta_6$ with an affinity that rivals that of antibodies. The increased affinity and stability of the tetrameric peptide opens the door for this peptide to be used as an *in vivo* reagent for targeted therapies of the treatment of aggressive $\alpha_v\beta_6$-positive tumors and molecular imaging.

Disclosure of Potential Conflicts of Interest

No potential conflicts of interest were disclosed.

[4] Y-H. Liu, M.J. McGuire, and K.C. Brown, unpublished results.

Acknowledgments

We thank Shaghayegh Rezaie, Sapna George, Jonathan Lee, and Naveen Pattisapu for technical assistance, and Bethany P. Gray for critical reading of the manuscript. This article represents publication no. CSCN036 from the Cell Stress and Cancer Nanomedicine Program of the Simmons Comprehensive Cancer Center.

References

1. Oyama T, Sykes KF, Samli KN, et al. Isolation of lung tumor specific peptides from a random peptide library: generation of diagnostic and cell-targeting reagents. Cancer Lett 2003;202:219–30.

2. Elayadi AN, Samli KN, Prudkin L, et al. A peptide selected by biopanning identifies the integrin $\alpha_v\beta_6$ as a prognostic biomarker for non-small cell lung cancer. Cancer Res 2007;67:5889–95.

3. Ahmed N, Riley C, Rice GE, Quinn MA, Baker MS. $\alpha_v\beta_6$ Integrin—a marker for the malignant potential of epithelial ovarian cancer. J Histochem Cytochem 2002;50:1371–9.

4. Breuss JM, Gallo J, DeLisser HM, et al. Expression of the b6 integrin in development, neoplasia, and tissue repair suggests a role in epithelial remodeling. J Cell Sci 1995;108:2241–51.

5. Kawashima A, Tsugawa S, Boku A, et al. Expression of av integrin family in gastric carcinomas: increased $\alpha_v\beta_6$ is associated with lymph node metastasis. Pathol Res Pract 2003;199:57–64.

6. Arihiro K, Kaneko M, Fujii S, Inai K, Yokosaki Y. Significance of $\alpha_9\beta_1$ and $\alpha_v\beta_6$ integrin expression in breast carcinoma. Breast Cancer 2000;7:19–26.

7. Jones J, Sugiyama M, Watt FM, Speight PM. Integrin expression in normal, hyperplastic, dysplastic, and malignant oral epithelium. J Pathol 1993;169:235–43.

8. Sipos B, Hahn D, Carceller A, et al. Immunohistochemical screening for β_6-integrin subunit expression in adenocarinomas using a novel monoclonal antibody reveals strong up-regulation in pancreatic ductal adenocarcinomas *in vivo* and *in vitro*. Histopathology 2004;45:226–36.

9. Hazelbag S, Kenter G, Gorter A, et al. Overexpression of the $\alpha_v\beta_6$ integrin in cervical squamous cell carcinoma is a prognostic factor for decreased survival. J Pathol 2007;212:316–24.

10. Bates RC, Bellovin DI, Brown C, et al. Transcriptional activation of integrin β_6 during the epithelial-mesenchymal transition defines a novel prognostic indicator of aggressive colon cancer. J Clin Invest 2005;115:339–47.

11. Breuss JM, Gillett N, Lu L, Sheppard D, Pytela R. Restricted distribution of integrin β_6 mRNA in primate epithelial tissues. J Histochem Cytochem 1993;41:1521–7.

12. Thomas GJ, Lewis MP, Whawell SA, et al. Expression of the $\alpha_v\beta_6$ integrin promotes migration and invasion in squamous carcinoma cells. J Invest Derm 2001;117:67–73.

13. Thomas GJ, Poomsawat S, Lewis MP, et al. $\alpha_v\beta_6$ integrin upregulates matrix metalloproteinase 9 and promotes migration of normal oral keratinocytes. J Invest Derm 2001;116:898–904.

14. Tam JP. Synthetic peptide vaccine design: synthesis and properties of a high density multiple antigenic system. Proc Natl Acad Sci U S A 1988;85:5409–13.

15. Tam JP. Recent advances in multiple antigen peptides. J Immunol Methods 1996;196:17–32.

16. Zhou X, Chang Y, Oyama T, McGuire MJ, Brown KC. Cell-specific delivery of a chemotherapeutic to lung cancer cells. J Am Chem Soc 2004;129:15656–7.

17. Bourel L, Carion O, Gras-Masse H, Melnyk O. The deprotection of Lys (Mtt) revisited. J Pept Sci 2000;6:264–70.

18. Oyama T, Rombel IT, Samli KN, Zhou X, Brown KC. Isolation of multiple cell-binding ligands from different phage displayed-peptide libraries. Biosens Bioelectron 2006;21:1867–75.

19. Kawakami T, Aimoto S, Nishimura T, Nakatsuji T, Sonobe H. Synthesis of cysteine-containing polypeptide using peptide thioester: preparation of a molt-inhibiting hormone from the American crayfish, *Procambarus clarkia*. Pept Sci 1999;35:149–52.

20. Duque H, Baxt B. Foot-and-mouth disease virus receptors: comparison of bovine α_v integrin utilization by type A and O viruses. J Virol 2003;77:2500–11.

Published OnlineFirst May 12, 2009; DOI: 10.1158/1535-7163.MCT-08-1098

21. Searle MS, Williams DH. The cost of conformational order-entropy changes in molecular associations. J Am Chem Soc 1992;114:10690–7.

22. Adams GP, Weiner LM. Monoclonal antibody therapy of cancer. Nat Biotech 2005;23:1147–57.

23. Kruger M, Beyer U, Shumacher P, et al. Synthesis and stability of four maleimide derivatives of the anticancer drug doxorubicin for the preparation of chemoimmunoconjugates. Chem Pharm Bull 1997;45:399–401.

24. Jaiswal JK, Mattoussi H, Mauro JM, Simon S. Long-term multiple color imaging of live cells using quantum dot bioconjugates. Nat Biotechnol 2003;21:47–51.

25. Davidson B, Dong HP, Holth A, NBerner A, Risberg B. Flow cytometric immunophenotyping of cancer cells in effusion specimens: diagnostic and research applications. Diagn Cytopathol 2007;35:568–78.

26. Torchilin VP, Lukyanov AN. Peptide and protein drug delivery to and into tumors: challenges and solutions. Drug Discov Today 2003;8:259–65.

27. Bracci L, Falciani C, Lelli B, et al. Synthetic peptides in the form of dendrimers become resistant to protease activity. J Biol Chem 2003; 278:46590–5.

28. Falciani C, Lozzi L, Pini A, et al. Molecular basis of branched peptides resistance to enzyme proteolysis. Chem Biol Drug Des 2007;69:216–21.

29. Arend L, Smart A, Brigga J. Mouse b6 integrin sequence, pattern of expression, and role in kidney development. J Am Soc Nephrol 2000;11: 2297–305.

30. Kraft S, Diedenbach B, Mehta R, et al. Definition of an unexpected ligand recognition motif for $\alpha_v\beta_6$ integrin. J Biol Chem 1999;274: 1979–85.

31. Goodman SL, Holzemann G, Sulyok G, Kessler H. Nanomolar small molecule inhibitors for $\alpha_v\beta_6$, $\alpha_v\beta_5$, and $\alpha_v\beta_3$ integrins. J Med Chem 2002;45:1045–51.

32. Weinreb P, Simon K, Rayhorn P, et al. Function-blocking integrin $\alpha_v\beta_6$ monoclonal antibodies: distinct ligand-mimetic and nonligand-mimetic classes. J Biol Chem 2004;279:17875–87.

33. Koopman Van Aarsen L, Leone D, Ho S, et al. Antibody-mediated blockade of integrin $\alpha_v\beta_6$ inhibits tumor progression *in vivo* by a transforming growth factor-b-regulated mechanism. Cancer Res 2008;68:561–70.

34. DiCara D, Rapisarda C, Sutcliffe JL, et al. Structure-function analysis of RGD-helix motifs in $\alpha_v\beta_6$ integrin ligands. J Biol Chem 2007;282: 9657–65.

35. Jackson T, Sheppard D, Denyer M, Blakemore W, King AM. The epithelial integrin $\alpha_v\beta_6$ is a receptor for foot-and-mouth disease virus. J Virol 2000;74:4949–56.

36. Sheppard D. Integrin-mediated activation of latent transforming growth factor b. Cancer Metastasis Rev 2005;24:395–402.

37. Hausner S, DiCara D, Marik J, Marshall JF, Sutcliffe JL. Use of a peptide derived from foot-and-mouth disease virus for the noninvasive imaging of human cancer: generation and evaluation of 4-[^{18}F]fluorobenzoyl A20FMDV2 for *in vivo* imaging of integrin $\alpha_v\beta_6$ expression with positron emission tomography. Cancer Res 2007;67:7833–7.

38. Aina OH, Liu R, Sutcliffe JL, et al. From combinatorial chemistry to cancer targeting peptides. Mol Pharmacol 2007;4:631–51.

39. Falciani C, Lozzi L, Pini A, Bracci L. Bioactive peptides from libraries. Chem Biol 2005;12:417–26.

40. Landon LA, Deutscher SL. Combinatorial discovery of tumor targeting peptides using phage display. J Cell Biochem 2003;90:509–17.

41. McGuire MJ, Sykes KF, Samli KN, et al. A library selected Langerhans cell-targeting peptide enhances an immune response. DNA Cell Biol 2004; 23:742–52.

42. De J, Chang Y, Samli KN, et al. Isolation of a *Mycoplasma*-specific binding peptide from an unbiased phage-displayed peptide library. Mol BioSyst 2005;1:149–57.

43. McGuire MJ, Samli KN, Chang Y, Brown KC. Novel ligands for cancer diagnosis: selection of peptide ligands for identification and isolation of B-cell lymphomas. Exp Hematol 2006;34:443–52.

44. Lozzi L, Lelli B, Runci Y, et al. Rational design and molecular diversity for the construction of anti-a-bungarotoxin antidotes with high affinity and *in vivo* efficiency. Chem Biol 2003;10:411–7.

45. Bracci L, Lozzi L, Pini A, et al. A branched peptide mimitope of the nicotinic receptor binding site is a potent synthetic antidote against the snake neutoxin a-bungarotoxin. Biochemistry 2002;41:10199.

46. Shin SY, Kaburaki Y, Watanabe M, Munekata E. Total solution synthesis of human epidermal growth factor by the assembly of 9 building-blocks. Biosci Biotechnol Biochem 1992;56:404–8.

47. Dawson PE, Muir TW, Clarklewis I, Kent SBH. Synthesis of proteins by native chemical ligation. Science 1994;266:776–9.

48. Rose K. Facile synthesis of homogeneous artificial proteins. J Am Chem Soc 1994;116:30–3.

49. Fisch I, Kunzi G, Rose K, Offord RE. Site-specific modification of a fragment of a chimeric monoclonal-antibody using reverse proteolysis. Bioconjug Chem 1992;3:147–53.

50. Liu CF, Tam JP. Chemical ligation approach to form a peptide-bond between unprotected peptide segments-concept and model study. J Am Chem Soc 1994;116:4149–53.

Published OnlineFirst May 12, 2009; DOI: 10.1158/1535-7163.MCT-08-1098

Molecular Cancer Therapeutics

Synthesis and characterization of a high-affinity $\alpha_v\beta_6$ -specific ligand for *in vitro* and *in vivo* applications

Shunzi Li, Michael J. McGuire, Mai Lin, et al.

Mol Cancer Ther 2009;8:1239-1249. Published OnlineFirst May 12, 2009.